Micron 43 (2012) 192–200

Contents lists available at ScienceDirect

Micron

journal homepage: www.elsevier.com/locate/micron

Alhydrogel® adjuvant, ultrasonic dispersion and protein binding: A TEM and analytical study

J. Robin Harris[a,b,*], Andrei Soliakov[a], Richard J. Lewis[a], Frank Depoix[b], Allan Watkinson[c,1], Jeremy H. Lakey[a,**]

[a] Institute for Cell and Molecular Biosciences, Newcastle University, Newcastle upon Tyne NE2 4HH, UK
[b] Institute of Zoology, University of Mainz, D-5509 Mainz, Germany
[c] PharmAthene UK, Billingham TS23 1YN, UK

ARTICLE INFO

Article history:
Received 26 April 2011
Received in revised form 10 July 2011
Accepted 11 July 2011

Keywords:
Alhydrogel
Aluminium hydroxide
Adjuvant
Vaccine
Ultrasonication
Protein binding
TEM
Negative staining
Cryo-TEM

ABSTRACT

Aluminium-based vaccine adjuvants have been in use since the 1920s. Aluminium hydroxide (alum) that is the chemical basis of Alhydrogel, a widely used adjuvant, is a colloid that binds proteins to the particular surface for efficient presentation to the immune system during the vaccination process. Using conventional TEM and cryo-TEM we have shown that Alhydrogel can be finely dispersed by ultrasonication of the aqueous suspension. Clusters of ultrasonicated aluminium hydroxide micro-fibre crystals have been produced (~10–100 nm), that are significantly smaller than those present the untreated Alhydrogel (~2–12 μm). However, even prolonged ultrasonication did not produce a homogenous suspension of single aluminium hydroxide micro-fibres. The TEM images of unstained and negatively stained air-dried Alhydrogel are very similar to those obtained by cryo-electron microscopy. Visualization of protein on the surface of the finely dispersed Alhydrogel by TEM is facilitated by prior ultrasonication. Several examples are given, including some of medical relevance, using proteins of widely ranging molecular mass and oligomerization state. Even with the smaller mass proteins, their presence on the Alhydrogel surface can be readily defined by TEM. It has been found that low quantities of protein tend to cross-link and aggregate the small Alhydogel clusters, in a more pronounced manner than high protein concentrations. This indicates that complete saturation of the available Alhydrogel surface with protein may be achieved, with minimal cross-linkage, and future exploitation of this treatment of Alhydrogel is likely to be of immediate value for more efficient vaccine production.

1. Introduction

Alhydrogel, an aqueous aluminium hydroxide (alum) suspension, has been reproducibly produced and widely used as a protein-binding vaccine adjuvant for many years (Bomford, 1980). Knowledge of the microcrystalline nature of this aluminium hydroxide product, its spontaneous aggregation and stability is well established, as is its marked immunostimulatory potential (Rostenberg et al., 2008). Alhydrogel is currently included in numerous patented vaccine formulations.

Industrial and pharmaceutical chemists have described a broad range of aluminium hydroxide and aluminium phosphate products (Demichelis et al., 2008; Edwards et al., 2009; Sato, 2007), characterized by chemical and physicochemical techniques, and by scanning electron microscopy (SEM) (Lee et al., 2009; Li et al., 2009, 2010; McLaughlin et al., 1993; Mortimer and Mayes, 2007) and transmission electron microscopy (TEM) (Burrell et al., 2001a,b; Chen et al., 2003; Counter et al., 1999; Hochepied et al., 2003; Wang et al., 2008). However, much uncertainty still remains as to the control of the Bayer crystallization process for the production of colloidal aluminium hydroxide crystalline suspensions. The protein-binding and adjuvant properties of aluminium salts have likewise been intensively studied (Clausi et al., 2008, 2009; Jones et al., 2005; Lindblad, 2004, 2006; Rinella et al., 1996), but with relatively little contribution from electron microscopy. Hem et al. have made numerous contributions to the aluminium based adjuvant field (*surveyed by* Hem et al., 2010; Hem and HogenEsch, 2007). Measurement of the protein content of Alhydrogel-based vaccines has recently been advanced by Zhu et al. (2009a,b) and the maintenance of secondary structure of proteins adsorbed by Alhydrogel was shown by Dong et al. (2006).

Ultrasonication of mineral particles has been widely used within chemical and materials science for the dispersion of the aqueous

* Corresponding author at: Institute for Cell and Molecular Biosciences, Newcastle University, Newcastle upon Tyne NE2 4HH, UK. Tel.: +44 01434 606981.
** Corresponding author.
E-mail addresses: rharris@uni-mainz.de (J.R. Harris), j.h.lakey@newcastle.ac.uk (J.H. Lakey).
[1] Current address: GSB Pharma, Guisborough TS14 6GG, UK.

0968-4328/$ – see front matter © 2011 Elsevier Ltd. All rights reserved.
doi:10.1016/j.micron.2011.07.012

suspensions of inorganic samples. In some cases these samples have been assessed by TEM or SEM (Chung et al., 2009; Janney et al., 2000; Li et al., 2007; Wu et al., 2011). Although aluminium hydroxide samples have not previously been treated by ultrasonication, aqueous suspensions of clustered alumina nanoparticles have been studied (Nguyen et al., 2011), indicating strongly the potential value of this approach. Whereas in the biomedical sciences water-bath and probe ultrasonicators are widely used, flow-through ultrasonication equipment is available which could readily extend the laboratory approach.

Although the safety and use of Alhydrogel vaccines is generally accepted, for example against malaria and anthrax (Campbell et al., 2007; Ellis et al., 2010; Mullen et al., 2006; Rostenberg et al., 2008; Sagara et al., 2009), the pathological deposition of aluminium hydroxide following injection has been shown by light and electron microscopy (Gherardi et al., 2001; Harris, 1973; Hernández et al., 2008; Valtulini et al., 2005).

Soliakov et al. (2010) studied by TEM the Caf1 polymer from the plague bacterium *Yersinia pestis*, anthrax protective antigen and hemocyanin that were each adsorbed to Alhydrogel. Although this work was the first to directly show proteins attached to Alhydrogel, a major limitation to the TEM work was the large size of the commercial Alhydrogel particles, which necessitated the selection of the rather few thin, partially electron-transparent, edges of the aluminium hydroxide microcrystalline clusters for data recording. We have now extended and facilitated our TEM study of several proteins adsorbed to Alhydrogel by producing controlled dispersion of the aluminium hydroxide by ultrasonication, using both water-bath and probe ultrasonication immediately prior to addition and adsorption of protein. We have also determined quantitatively the protein adsorption of this more finely dispersed ultrasonicated Alhydrogel, compared to the untreated aqueous Alhydrogel dispersed by manual mixing.

2. Materials and methods

2.1. Alhydrogel

AlhydrogelTM, a 2% (w/v) aqueous suspension of aluminium hydroxide gel adjuvant, was purchased from BRENNTAG Biosector, Frederikssund, Denmark (Batch No. 4072).

2.2. Proteins

Recombinant anthrax protective antigen (PA83), the plague bacterium *Yersina pestis* capsular antigen fraction 1 (Caf1) (Miller et al., 1998; Zavialov et al., 2003) and the LcrV injectisome tip antigen (Mueller et al., 2005; Broz et al., 2007) were provided by Avecia Biologics Ltd. (UK). The PA83 was converted proteolytically to PA63, which oligomerizes as the stable heptamer (Petosa et al., 1997). Recombinant respiratory syncytial virus nucleocapsid protein-RNA (RSV N-RNA) decamer was purified by established procedures (MacLellan et al., 2007; Tawar et al., 2009). The *E. coli* outer membrane porin OmpF trimer (Yamashita et al., 2008) was purified by the method of Gravito and Rosenbusch (1986). Horse spleen ferritin, apoferritin and keyhole limpet hemocyanin (KLH) were purchased from Sigma Aldrich, and collagen (acid-soluble, rat tail type I) from SERVA Electrophoresis. Recombinant enolase from *Bacillus subtilis* was prepared as described by Newman et al. (in preparation). Sedimentation velocity and size exclusion chromatography indicated that the enolase was octameric, as with some other bacterial enolases (Schurig et al., 1995). Proteins were added to water-diluted Alhydrogel suspensions (0.1 mg/ml), at concentrations ranging from 0.01 to 0.1 mg/ml. In general, over saturation of the available Alhydrogel surface with protein was avoided, as the presence of excess unbound protein does not assist the subsequent interpretation of the TEM images. However, undersaturation leads to aggregation of the Alhydrogel particles due to protein cross-linkage.

2.3. Ultrasonication of Alhydrogel

The 2% stock solution of Alhydrogel was thoroughly hand-mixed and routinely diluted to 5 μl/ml in distilled water (giving ~0.1 mg/ml) prior to ultrasonication. Ultrasonication was performed at room temperature using 50 ml samples in a water-bath ultrasonicator (Grant XB2, Cambridge, UK) and as ice-cooled 2 ml volumes using a probe ultrasonicator (Misoix Sonicator 3000, USA) with a microtip probe at intensity setting 1.5, with 15/10 s on/off time ultrasonication and cooling cycles.

2.4. Determination of protein binding

The protein-adjuvant mixtures were centrifuged at 3000 × *g* for 3 min at room temperature. The supernatants were removed and assessed for protein concentration by measuring the absorbance at 280 nm. The amount of protein adsorbed to aluminium hydroxide adjuvant at room temperature was calculated by subtracting the amount of protein remaining in solution from the amount of protein added initially (Jones et al., 2005).

2.5. Specimen preparation for electron microscopy

Specimens were prepared on carbon-coated and holey carbon-coated 400 mesh copper EM grids. Grids were briefly treated (60 s) by glow discharge to improve their hydrophilicity. EM specimens were prepared on the continuous carbon films, unstained and negatively stained with 2% (w/v) aqueous uranyl acetate, using the single droplet procedure (Harris, 1997). Specimens were prepared on holey carbon films, unstained in 1% (w/v) aqueous trehalose and negatively stained with 5% aqueous (w/v) ammonium molybdate, 0.1% (w/v) trehalose (pH 6.9), as described by Harris and Scheffler (2002). Frozen hydrated specimens were on holey films by the plunge-freezing procedure of Adrian et al. (1984), with a user-modified Gatan Cp3. 300 Mesh C-Flat grids with 2 μm holes at 2 μm spacing were used, without glow discharge.

2.6. Transmission electron microscopy

TEM study was performed at ambient temperature using a Philips CM100, at 100 kV. Digital images were recorded using an Optronics 1824 × 1824 pixel CCD camera with an AMT40 version 5.42 image capture engine, supplied by Deben UK. Cryoelectron microscopy was performed using a Tecnai 12 BioTwin, with a Tvips TemCam F416 (4 k × 4 k) CCD camera. Digital image compilation for publication was performed in Photoshop.

3. Results

3.1. Alhydrogel before ultrasonication

Alhydrogel readily binds to carbon support films, which enables rapid water washing to be performed to remove any soluble salt, which might otherwise dry alongside the aluminium (oxy)hydroxide crystals. The inherent mass thickness (density × thickness) of the thinly spread mineral then renders electron imaging possible, albeit following dehydration within the high vacuum of the TEM. Untreated alhydrogel has been found to consist of large clusters of micro-fibre primary crystallites (~2–12 μm), which self-associate following manual mixing and

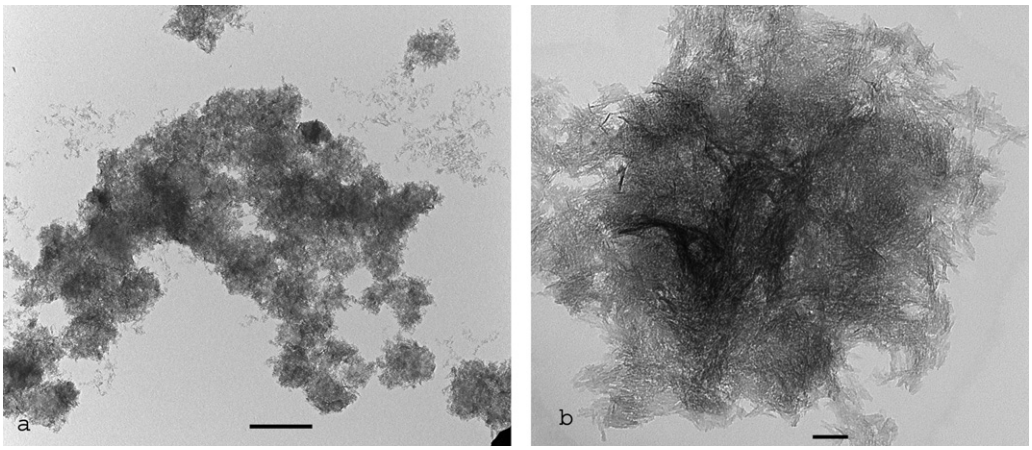

Fig. 1. TEM images of untreated Alhydrogel imaged without staining, (a) at low magnification and (b) higher magnification. Note the excessive electron density of these large Alhydrogel micro-crystalline clusters (~2–12 μm), which precludes detailed structural assessment of protein-binding. The scale bars indicate 2 μm (a) and 100 nm (b).

sediment under unit gravity. These properties account for the gel-like nature of the 2% suspension of Alhydrogel. Fig. 1a shows a representative TEM image of an unstained untreated Alhydrogel. Because of the thickness of the crystal clusters it is not possible to define individual micro-fibrils, except at the relatively few regions where the cluster edge is thin (Fig. 1b), as also encountered by Soliakov et al. (2010).

3.2. Alhydrogel after ultrasonication

Following treatment of Alhydrogel with relatively gentle water-bath ultrasonication (5, 10 and 30 min) in a Grant XB2 it is clear that the size of the micro-crystal clusters decreases (~50–300 nm), as shown in Fig. 2 when imaged without staining and when negatively stained with uranyl acetate. Despite the treatment, most of the individual aluminium hydroxide micro-crystals still tend to be associated together as small clusters. Similarly, when more powerful ultrasonication was applied using Misoix Sonicator 3000 with a titanium microtip probe (5 and 10 min), with an intensity setting of 1.5, the aluminium hydroxide micro-crystal clusters dispersed markedly (~10–100 nm). In these instances it became possible to define some very small, almost individual microcrystals (Fig. 3a). Extension of the treatment to 30 min produced larger numbers of small micro-crystal clusters, but still relatively few individual micro-fibres, indicating the strong association of the aluminium hydroxide microfibres during their chemical formulation and initial crystallization. Optimal spreading of the Alhydrogel micro-crystals is necessary to avoid superimposition of crystals, which might otherwise suggest the presence of larger clusters. When spread across the holes of holey carbon support films in the presence of 1% trehalose, the ultrasonicated Alhydrogel was again revealed by its inherent electron scattering power (Fig. 3b), larger particles having a tendency to be located towards the edge of the holes, where the dried trehalose film is slightly thicker. A similar situation occurs during the preparation of unstained frozen-hydrated specimens (Fig. 3c and d). If the Alhydrogel is present at a greater than optimal concentration, superimposition of small particles readily occurs when the material is adsorbed to carbon support films and also when spread in solution across holes. This can readily be avoided by varying the specimen preparation/dilution conditions. Remarkably, following the probe ultrasonication treatment, little reaggregation of the small aluminium hydroxide micro-crystal clusters was found to occur over a period of weeks. Even though sedimentation under unit gravity does occur, resuspension of the Alhydrogel particles by manual mixing is relatively efficient.

3.3. Analysis of protein binding to Alhydrogel

Determination of the quantity of protein bound to untreated and ultrasonicated Alhydrogel by established procedures did not reveal a difference. The binding isotherms and Langmuir regressions showed similar binding capacity for the untreated and ultrasonicated Alhydrogel (see Supplementary Material).

3.4. Ultrasonicated alhydrogel with adsorbed proteins

The binding of several proteins to Alhydrogel has been studied by TEM. Some of the selected proteins (Table 1) have direct relevance for experimental vaccine production: (anthrax protective antigen PA83 and PA63, *Yersinia pestis* capsular Caf1 antigen and LcrV antigen, *E. coli* outer membrane protein OmpF and human respiratory syncytial virus nucleocapsid protein-RNA (RSV n-RNA). Other proteins are purely of technical interest, to demonstrate the inherent ability of Alhydrogel to bind to any protein. In this regard, ferritin and apoferrtin provide useful examples, owing to the presence and absence of the iron hydroxide core, respectively, within an essentially spherical hollow oligomeric ~11 nm diameter 24mer protein shell. Whilst keyhole limpet hemocyann (KLH) has been widely used as an adjuvant and antigen carrier in its own right (Harris and Markl, 1999), it is a relevant high molecular mass protein for the present study.

A general observation has been that with all the proteins studied, it has been necessary to add sufficient protein to produce saturation of the binding capacity of the Alhydrogel in order to prevent subsequent aggregation produced by cross-linkage of the Alhydrogel particles (essentially equivalent to immune complex formation). Dependent upon the protein mass and oligomerization state, together with the concentration of Alhydrogel suspension present and the state of dispersal, the necessary protein concentration will vary. All the above-mentioned proteins have been studied

Table 1
Proteins used in this study.

Ferritin (24mer ~241 kDa + iron hydr/oxide core)
Apoferritin (24mer ~241 kDa)
Keyhole limpet hemocyanin KLH (didecamer ~9 MDa
Anthrax protective antigen PA63 (heptamer ~440 kDa)
Respiratory syncytial virus nucleocapsid protein RSV n-RNA (decamer ~430 kDa)
E. coli outer membrane porin OmpF (trimer ~120 kDa)
Rat tail collagen type 1 (heterotrimer ~300 kDa)
Yersinia pestis capsular antigen Caf1 (monomer ~15.5 kDa and linear polymers)
Yersinia pestis LcrV antigen (monomer ~37 kDa and pentamer)
Bacillus subtilis enolase (octamer ~345 kDa)

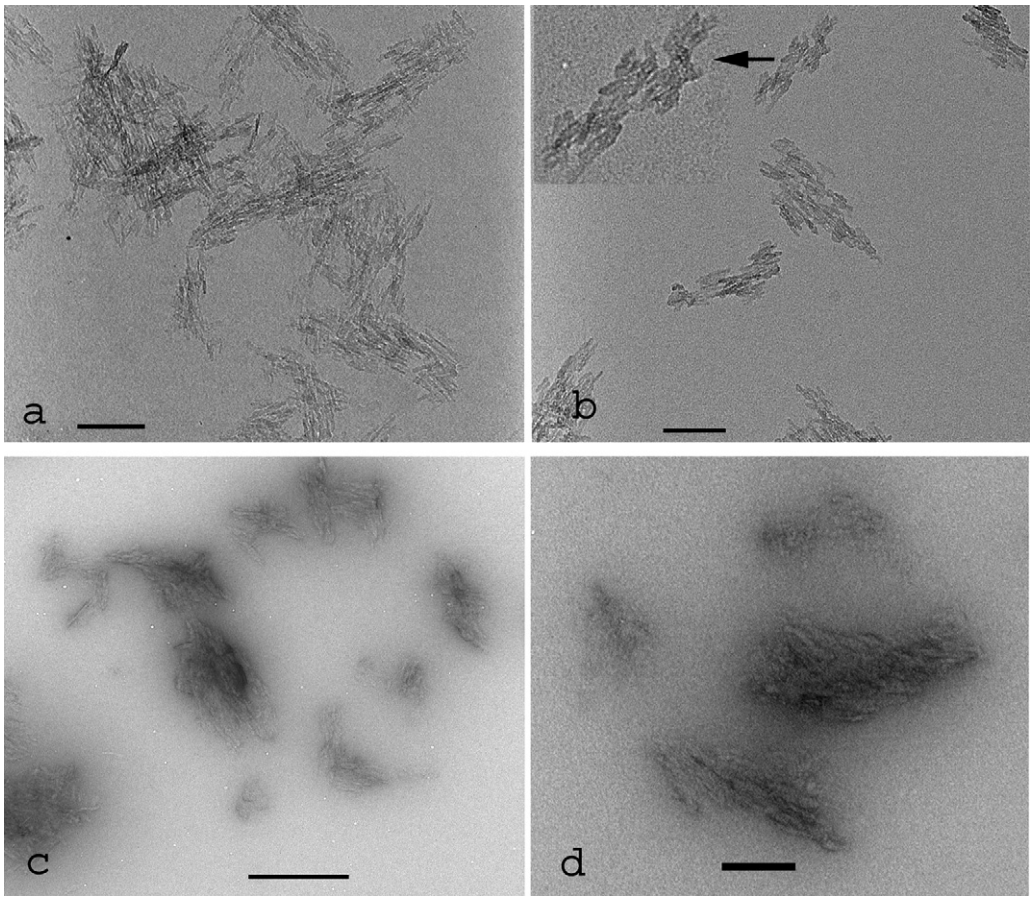

Fig. 2. TEM images of Alhydrogel following ultrasonication in a water-bath sonicator for 10 min. (a, b) Images of unstained Alhydrogel (inset b, at higher magnification), and (c, d) Alhydrogel negatively stained with uranyl acetate. Note that the Alhydrogel clusters (~50–300 nm) are significantly smaller than those shown in Fig. 1. The scale bars indicate 100 nm.

by TEM in the presence of the negative stain uranyl acetate, which readily reveals the surface coating of protein on the Alhydrogel. Ferritin molecules bound to Alhydrogel have also been imaged in the absence of negative stain.

3.4.1. Ferritin and apoferritin

Horse spleen ferritin has been imaged by TEM in the absence of negative stain, revealed electron optically by the presence of the iron (hydr)oxide core, and when surrounded by negative stain, when both metallic core and protein shell are revealed. Fig. 4 shows TEM images of ferritin adsorbed to ultrasonicated Aldydrogel in the absence of stain (Fig. 4a–c) and in the presence of uranyl acetate negative stain (Fig. 4d). Essentially equivalent negatively stained images of negatively stained apoferritin (devoid of metallic core) when bound to Alhydrogel are shown in Fig. 4e.

3.4.2. Keyhole limpet hemocyanin KLH, anthrax protective antigen PA63 heptamer, respiratory syncytial virus nucleocapsid protein RSV n-RNA decamer and E. coli outer membrane porin OmpF trimer

Keyhole limpet hemocyanin occurs as two isoforms (KLH1 and KLH2), which form higher oligomers of a stable decameric unit. The didecamer tends to predominate for both isoforms, but KLH2 also forms elongated multidecamers (Harris and Markl, 1999). We have used the unfractionated hemocyanin, thus containing a mixture of KLH1 and KLH2 decameric and higher multidecameric forms. When adsorbed to Alhydrogel, the KLH multimers are readily defined when attached to the ultrasonicated samples (Fig. 5a). Similarly, individual anthrax PA63 heptamers and RSV n-RNA decamers can be defined on the Alhydrogel surface (Fig. 5b and c), but the smaller mass OmpF trimer can only be detected as a relatively smooth coating on the Alhydrogel (Fig. 5d).

3.4.3. Yersinia pestis Caf1, Yersinia pestis LcrV, rat tail collagen type 1 heterotrimer and B. subtillis enolase octamer

The plague bacterium *Yersinia pestis* Caf1- and LcrV-antigens are both of considerable interest with respect to vaccine production. When bound to ultrasonicated Alhydrogel the Caf1 polymers thickly coat the Alhydrogel surface, but the beaded polymer chains can also be seen to extend from the surface (Fig. 6a). On the other hand, the smaller mass LcrV-antigen can only be assessed as a smooth coating on the Alhydrogel (Fig. 6b), without clear definition of the monomer or pentamer. The thin elongated ~300 kDa collagen type 1 heterotrimer, which cannot be easily defined by negative staining, is revealed as a beaded coating on the Alhydrogel (Fig. 6c), with molecules extending from the surface. *Bacillus subtilis* enolase readily coats the Alhydrogel particles (Fig. 6d), again with some unbound molecules and possibly dissociated molecules. Perhaps not surprisingly, the mesophilic *B. subtilis* enolase octamer appears to be less stable than that from the hyperthermophilic bacterium *Thermotoga maritima* (Shurig et al., 1995).

4. Discussion

Aluminium-based adjuvants have been in use since the early 1920s, when Glenny et al. (1926) produced an alum precipitation of diphtheria toxoid which was an effective vaccine. Through the following decades, extensive analysis of aluminium hydroxide

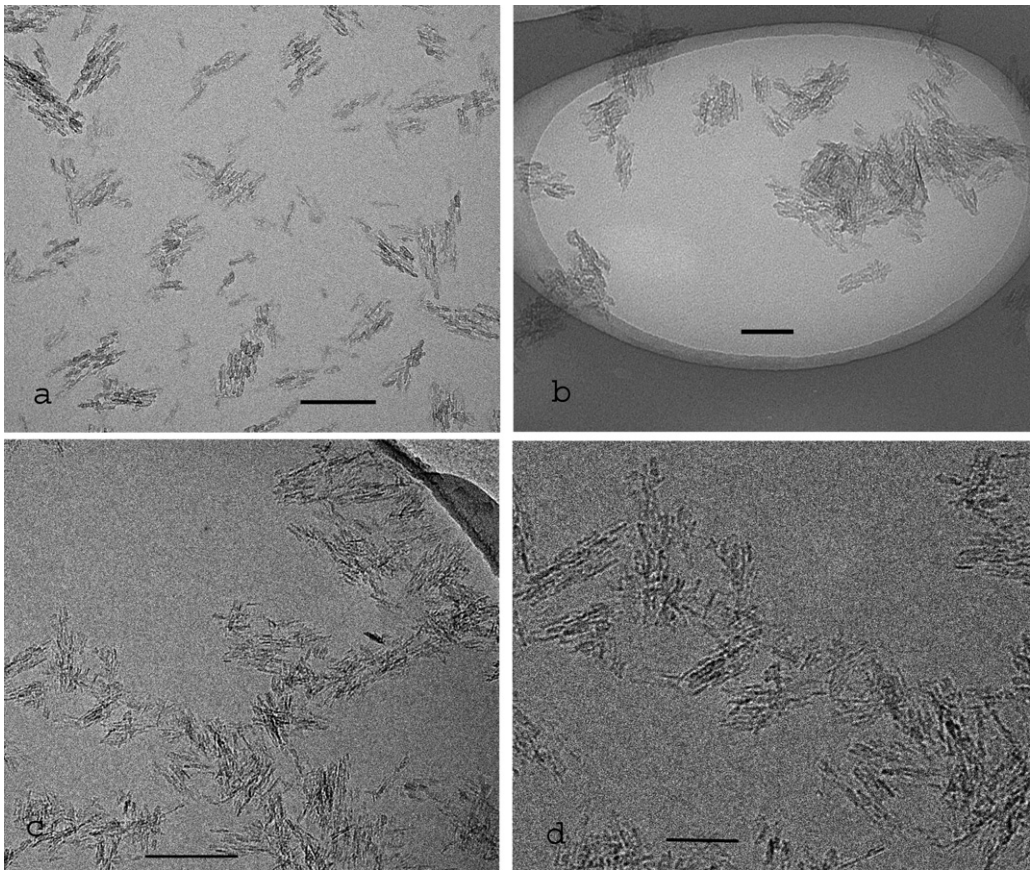

Fig. 3. TEM images of Alhydrogel following ultrasonication with a probe sonicator for 10 min (intensity setting 1.5). Note the marked increase in the number of very small Alhydrogel microfibre clusters (~10–100 nm). The samples were (a) unstained and adsorbed to a carbon support film, (b) spread in the presence of 1% trehalose across the holes of a holey carbon support film and (c, d) frozen-hydrated (with some aggregation or superimposition of the finely dispersed Alhydrogel). The scale bars indicate 100 nm (a–c) and 50 nm (d).

adjuvants was performed. Although the detailed structural nature of the various products was not studied greatly, they were used widely for the preparation of vaccines, the properties of which were intensively studied *in vivo* with respect to the immunogenicity of the final vaccine product. Certainly, the biological and biochemical properties of protein antigens were studied, but the available aluminium hydroxide carrier was used in a standard form without additional particle size or aggregation analysis, or further treatment. However, in recent years it has become a pharmaceutical requirement that all the components of a vaccine formulation should be studied individually, as well as the final product. Study of the properties of proteins desorbed from aluminium hydroxide has been one approach, but additional methods are necessary to establish fully the properties of vaccines and their components. The highly defined protein substance which is combined with the adjuvant can be characterised using electrophoretic, spectroscopic and other procedures. It is clear that the three dimensional protein polymer may undergo structural changes when bound tightly to a solid surface such as Alhydrogel. However the changes are difficult to measure since most methods used in protein structure determination require pure proteins in solution. We have recently developed a range of techniques to address this problem but even so, resolving the three dimensional structures of bound proteins is difficult. In this respect electron microscopy has made a significant contribution by providing clear images of Alhydrogel-bound molecules.

The Alhydrogel adjuvant used in this study has been shown to possess a fine fibre-like micro-crystalline substructure (Figs. 1–3). These images are in general accord with those shown Shirodkar et al. (1990) using untreated Alhydrogel and by Dabbagh et al. (2011) for clusters of alumina nanorods, but are at variance for many of the thin platelet, spherical or disordered micro-crystalline preparations of aluminium hydroxide produced by others (Chen et al., 2003; Counter et al., 1999; Hochepied et al., 2003; Li et al., 2009; Mortimer and Mayes, 2007; Wang et al., 2008). This structural variability underlines the different chemical procedures and processes used for producing aluminium hydroxide products in industry, many of which are not utilized for vaccine production.

The progressive dispersion of Alhydrogel clusters by ultrasonication has been shown to be reproducible, and to be intensity- and time-dependent, although the production of a homogeneous aqueous suspension of single very small uniformly sized fibrillar primary crystallites of aluminium hydroxide has not yet been achieved. A similar outcome was shown by Nguyen et al. (2011) by ultrasonicating nanoscale alumina particles; they commented on the fact that excessive ultrasonication carried a risk of producing reagglomeration. Nevertheless, the production of smaller crystalline microfiber clusters of Alhydrogel has enabled a more detailed TEM study of protein attachment to be performed, by avoiding the excessive image density and subsequent lack of detail imparted by the larger untreated Alhydrogel clusters (Soliakov et al., 2010). Comparison of the cryoTEM data of unstained ultrasonicated Alhydrogel with that obtained by conventional TEM of unstained stained samples spread on carbon support films and spread as a thin film across holes in the presence of trehalose, indicates that all are essentially the same, and therefore mutually supportive. This is despite the fact that dehydration of the aluminium hydroxide crystals will occur

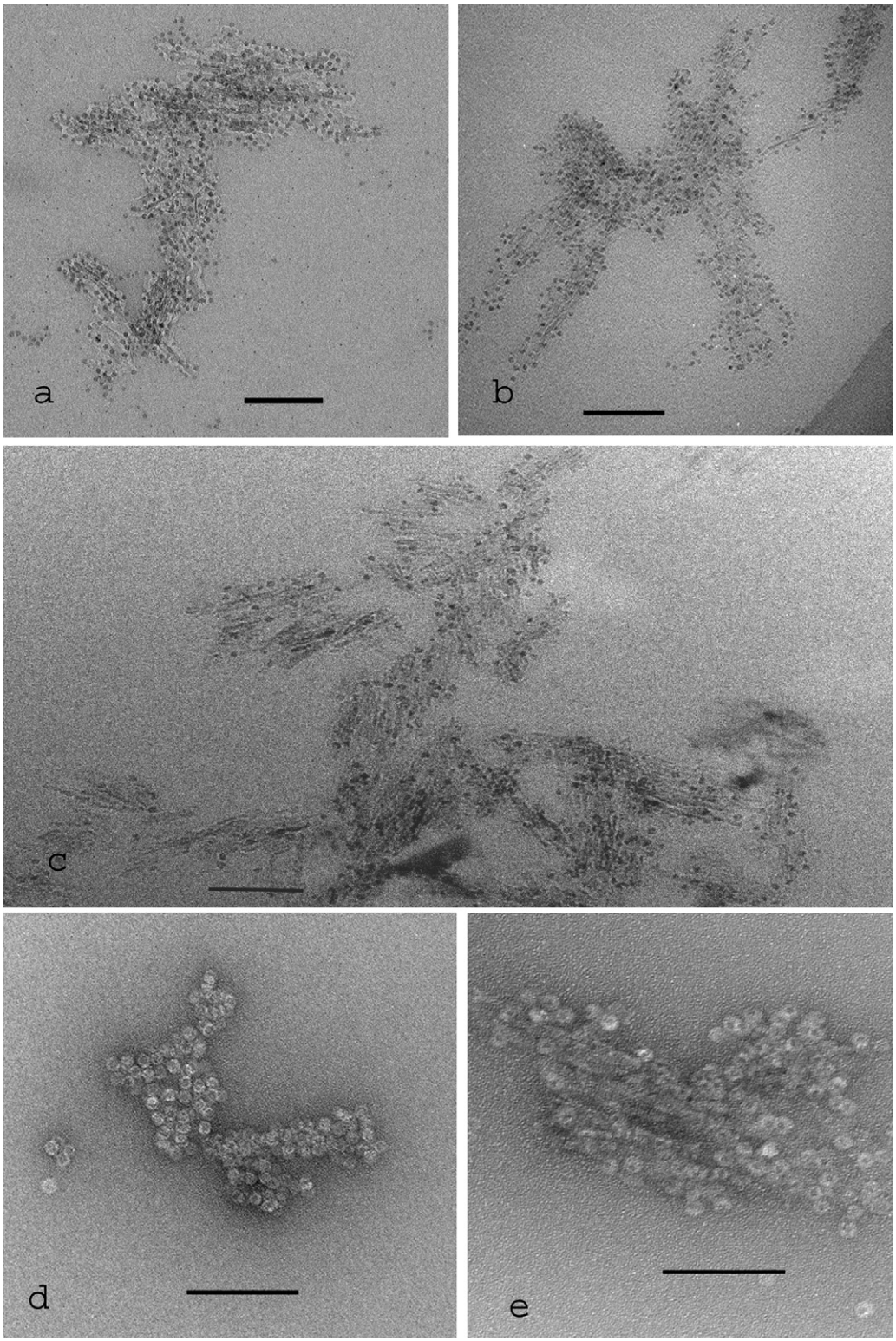

Fig. 4. TEM images of ultrasonicated Alhydrogel with adsorbed ferritin and apoferritin molecules. The ferritin-adjuvant complex is shown (a) unstained bound to a carbon support film, (b) freely spread across a hole in the presence of trehalose and (c) frozen-hydrated. Representative examples of (d) ferritin and (e) apoferritin adsorbed onto the surface of Alhydrogel, negatively stained with uranyl acetate. The scale bars indicate 100 nm (a, b, d, e) and 50 nm (c).

during intra-TEM evacuation of the specimen grid and subsequent electron imaging. Overall, we show the value of TEM for the qualitative assessment of protein binding by Alhydrogel. This approach could also be useful for the study of freeze-thawed and freeze-dried aluminium hydroxide-containing vaccines (Solanki et al., 2011; Wolff et al., 2008).

Johnston et al. (2002) measured the available surface area of aluminium hydroxide adjuvant for protein binding as 514 m^2/g. It might reasonably be predicted that dispersion of the Alhydrogel would increase the available surface area for protein binding, in turn leading to an increased quantity of protein bound to Alhydrogel. Our available data (*see* Supplementary data Figs. S1–S4) does

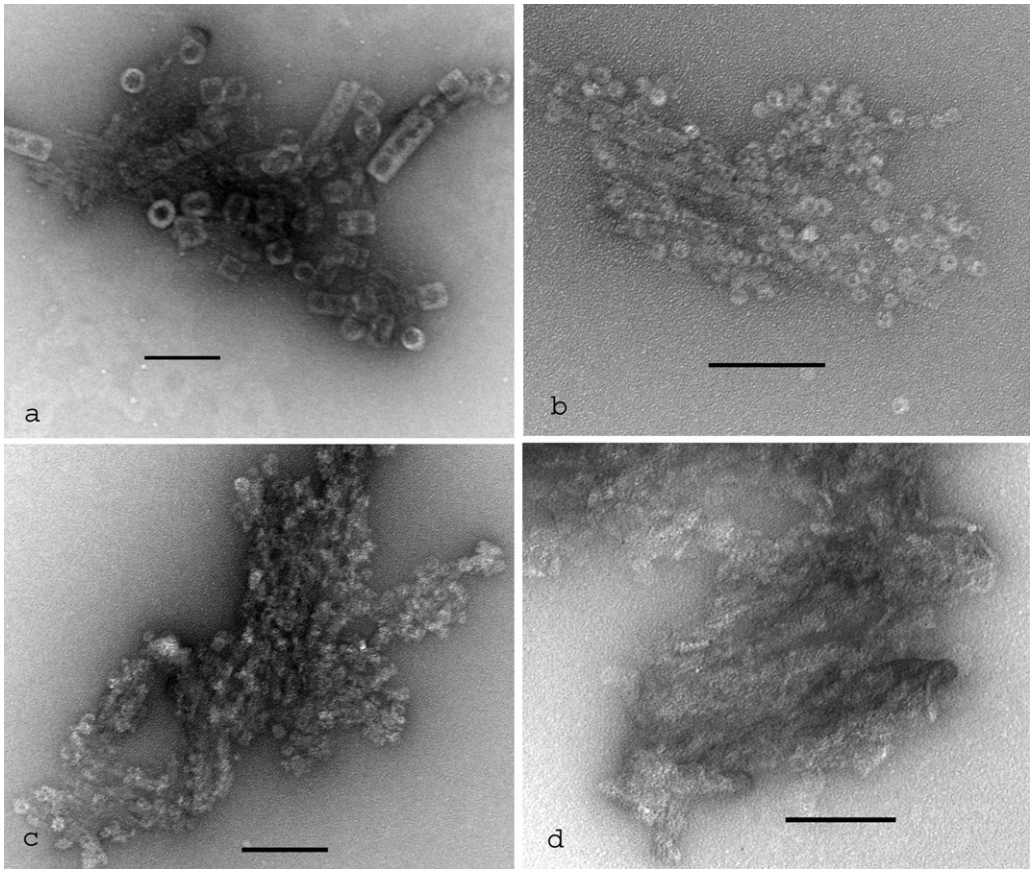

Fig. 5. TEM images of negatively stained ultrasonicated Alhydrogel with adsorbed proteins. (a) Keyhole limpet hemocyanin, (b) anthrax protective antigen PA63, (c) respiratory syncytial virus nucleocapsid protein RSV n-RNA and (d) *E. coli* outer membrane protein OmpF. The scale bars indicate 100 nm.

not show any increase, possibly because of the diffuse nature of the untreated Alhydrogel micro-fibre clusters, which enables protein access to the internal surfaces within the clusters, although this would be likely to vary depending upon the protein mass. A factor that could have skewed the analytical data from the ultrasonicated Alhydrogel is the observation that at sub-maximal binding there is cross-linkage of the Alhydrogel particles due to the available unsaturated aluminium hydroxide surface. This protein bridging is likely to be more marked with the finely dispersed Alhydrogel, resulting in an inaccurate figure for the amount of bound protein per mg of Alhydrogel. Nevertheless, cross-linked material may provide a prolonged exposure to bound antigens resulting in a stronger stimulation of the *in vivo* immune response, but this remains to be experimentally proven. The protein-induced aggregation of small particles of Alhydrogel produced by ultrasonication can be avoided if the Alhydrogel is initially adsorbed to a carbon support film, followed by the addition of protein. Our preliminary data indicates that this is the case (Supplementary Fig. S5), the problem here being the inevitable presence of some unbound protein on the carbon support film. Blockage of the adsorption properties of the carbon film, without blocking the adsorptive capacity of Alhydrogel, using a soluble neutral compound such as low mass PEG or a disaccharide is possible, but has not so far proved to be successful.

Our TEM data shows that all the proteins tested adsorb strongly to Alhydrogel, due to the nascent aluminium cationic charge that rapidly binds proteins possessing a net negative charge. Positively charged proteins bind more readily to phosphate-saturated Alhydrogel ($AlPO_4$) (Burrell et al., 2001a, b; Jones et al., 2005). Depending upon the mass and oligomerization state of any protein under investigation by TEM, it may or may not be possible to clearly define structurally an individual protein at the edge of a small Alhydrogel micro-crystal cluster. Undersaturation with protein as assessed by TEM will usually be obvious, particularly the occupancy by larger proteins, and exceeding the Alhydrogel binding capacity will be shown by the presence of free protein molecules. Image superimposition of protein bound to the upper and lower Alhydrogel surface will occur in all cases, only the protein molecules bound around the edges being clearly defined. In addition, the overall orientation of the bound proteins is shown to be extremely variable. The mass difference selected for the proteins range from ~15.5 kDa for the *Yersinia pestis* Caf1 monomer to upwards of ~9 MDa for KLH (depending upon the multimeric state of the KLH decamer, the didecamer being the predominant species). It is clear that with the large oligomeric proteins, a greater amount of protein surface and therefore number of specific epitopes could be exposed on the surface of the mineral adjuvant than might be the case with a monomeric coating of a protein of smaller mass. Elongated proteins bound to Alhydrogel, such as the Caf1 oligomer and the soluble collagen heterotrimer, are likely to expose significant lengths of unattached protein (Soliakov et al., 2010). Whether or not these considerations could be reflected in terms of immunogenicity is not known and has not been assessed in the present study. However, it is clear from our structural data that proteins bound to Alhydrogel do not suffer any significant deformation, except possibly at the sites of direct interaction between the protein amino acid carboxyl side chains to the Alhydrogel.

Many of the test proteins selected this study are currently under structural investigation in our laboratory (Caf1, LcrV, RSV n-RNA, OmpF, PA63, enolase), or have been previously handled by us (ferritin, apoferritin, KLH, collagen type 1). KLH and other molluscan hemocyanins (Gesheva et al., 2011; Guo et al., 2011) are established hapten carriers and immunostimulants (Harris and Markl,

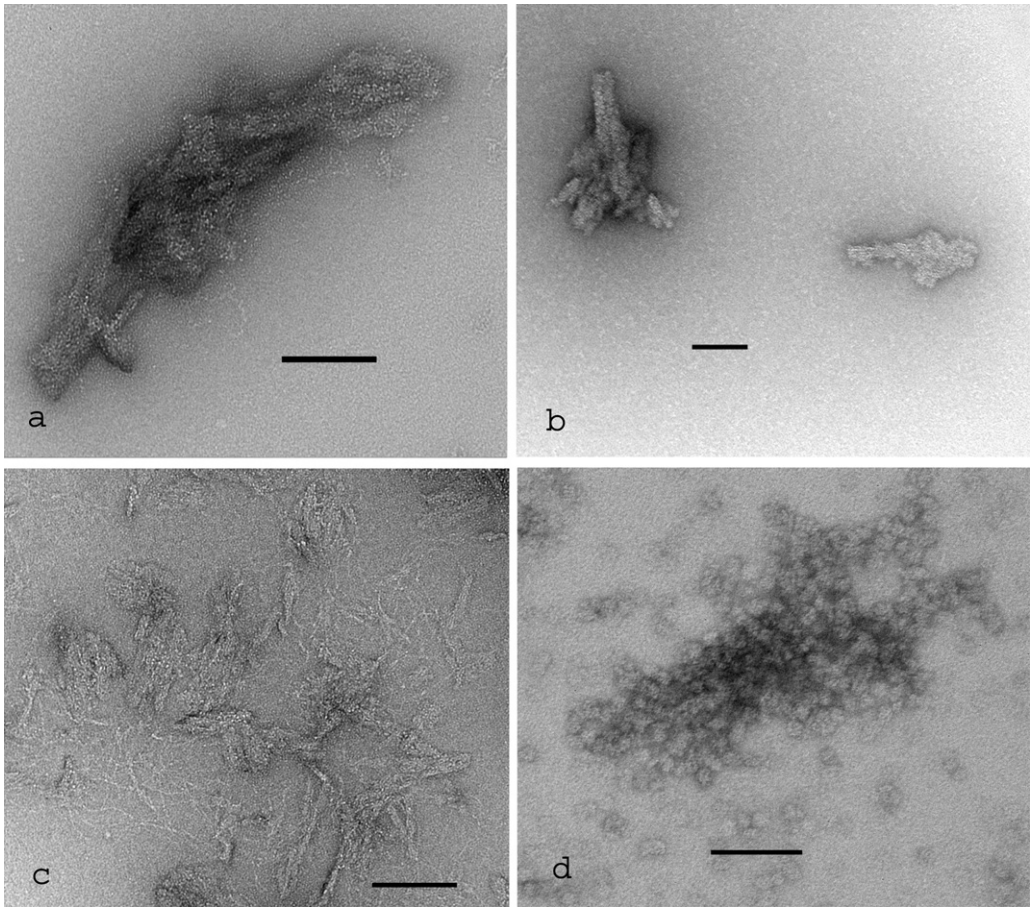

Fig. 6. TEM images of negatively stained ultrasonicated alhydrogel with adsorbed proteins. (a) *Yersinia pestis* Caf1, (b) *Yersinia pestis* V-antigen, (c) acid-soluble rat tail collagen type 1 heterotrimer and (d) *Bacillus subtilis* enolase octamer. The scale bars indicate 100 nm.

1999; Presicce et al., 2008; Zhang et al., 2010) and may be of further interest within the context of adjuvant cocktails, since their use in conjunction with Alhydrogel could enhance the immune response.

We believe that many proteins and peptides of clinical interest for vaccine production would, due to the powerful protein-binding properties of aluminium hydroxide, be definable by TEM on the surface of Alhydrogel, thus providing an addition to quality assessment. Consequently, it may be of use to the biopharmaceutical industry involved in human and animal vaccine production as a tool for screening their final products and where appropriate the vaccine components, alongside other established quality assessment/assurance procedures. In addition, we believe that size control of the Alhydrogel adjuvant can be assessed by TEM and that ultrasonication could readily be used on an industrial-scale (e.g. Leonelli and Mason, 2010) to produce controlled dispersion of this adjuvant prior to the addition of any protein antigen. Although this might involve changes in the formulation process for vaccines it may, in the long term, provide advantages in protein binding density, vaccine potency and product homogeneity, but this remains to be demonstrated.

Acknowledgements

Financial support to AS during this work was received from the BBSRC for a CASE studentship award. We wish to thank Avecia Biotechnology and Pharmathene for support, and the Electron Microscopy Research Services facility at Newcastle University for expertise and equipment. Access to cryoEM facilities was provided by Prof. Dr J. Markl, Institute of Zoology, University of Mainz.

Appendix A. Supplementary data

Supplementary data associated with this article can be found, in the online version, at doi:10.1016/j.micron.2011.07.012.

References

Adrian, M., Dubochet, J., Lepault, J., McDowall, A.W., 1984. Cryo-electron microscopy of viruses. Nature 308, 32–36.

Bomford, R., 1980. The comparative selectivity of adjuvants for humoral and cell-mediated immunity. I. Effect on the antibody response to bovine serum albumin and sheep red blood cells of Freund's incomplete and complete adjuvants, alhydrogel, Corynebacterium parvum, Bordetella pertussis, muramyl dipeptide and saponin. Clin. Exp. Immunol. 39, 426–434.

Broz, P., Mueller, C.A., Müller, S.A., Philippsen, A., Sorg, I., Engel, A., Cornelia, G.R., 2007. Function and molecular architecture of the *Yersina* injectisome tip complex. Mol. Microbiol. 65, 1311–1320.

Burrell, L.S., Johnston, C.T., Schulze, D., Klein, J., White, J.L., Hem, S.L., 2001a. Aluminium phosphate adjuvants prepared by precipitation at constant pH. Part II: physicochemical properties. Vaccine 19, 275–281.

Burrell, L.S., Johnston, C.T., Schulze, D., Klein, J., White, J.L., Hem, S.L., 2001b. Aluminium phosphate adjuvants prepared by precipitation at constant pH. Part II: physicochemical properties. Vaccine 19, 282–287.

Campbell, J.D., Clement, K.H., Wasserman, S.S., Donegan, S., Chrisley, L., Kotloff, K.L., 2007. Safety, retroactivity and immunogenicity of a recombinant protective antigen vaccine given to healthy adults. Hum. Vaccin. 3, 205–211.

Chen, J.-F., Shao, L., Guo, F., Wang, X.-M., 2003. Synthesis of nano-fibers of aluminium hydroxide in novel rotating packed bed reactor. Chem. Eng. Sci. 58, 569–575.

Chung, S.J., Leonard, J.P., Nettleship, I., Lee, J.K., Soong, Y., Martello, D.V., Chyu, M.K., 2009. Characterization of ZnO nanoparticle susupension in water: effectiveness of ultrasonic dispersion. Powder Technol. 194, 75–80.

Clausi, A., Cummiskey, J., Merkley, S., Carpenter, J.F., Braun, L.J., Randolph, T.W., 2008. Influence of particle size and antigen binding on effectiveness of aluminium salt adjuvants in a model lysozyme vaccine. J. Pharm. Soc. 97, 5252–5262.

Clausi, A.L., Morin, A., Carpenter, J.F., Randolph, T.W., 2009. Influence of protein conformation and adjuvant aggregation on the effectiveness of aluminium

hydroxide adjuvant in a model alkaline phosphatase vaccine. J. Pharm. Soc. 98, 114–121.
Counter, J.A., Addai-Mensah, J., Ralston, J., 1999. The formation of $Al(O)_3$ crystals from supersaturated sodium aluminate solutions revealed by cryovitrification-transmission electron microscopy. Colloids Surf., A 154, 389–398.
Dabbagh, H.A., Rasti, E., Yalfani, M., Medina, F., 2011. Formation of γ-alumina rods in the presence of alanine. Mater. Res. Bull. 46, 271–277.
Demichelis, R., Civalleri, B., Noel, Y., Meyer, A., Dovesi, R., 2008. Structure and stability of aluminium trihydroxides bayerite and gibbsite: a quantum mechanical *ab initio* study with the CRYSTA06 code. Chem. Phys. Lett. 465, 220–225.
Dong, A., Jones, L.S., Kerwin, B.A., Krishnan, S., Carpenter, J.R., 2006. Secondary structures of proteins adsorbed onto aluminium hydroxide: infrared spectroscopic analysis of proteins from low solution concentrations. Anal. Biochem. 351, 282–289.
Edwards, I., Axon, S.A., Barigou, M., Stitt, E.H., 2009. Combined use of PEPT and ERT in the study of aluminium hydroxide precipitation. Ind. Eng. Chem. Res. 48, 1019–1028.
Ellis, R.D., Martin, L.B., Shaffer, D., Long, C.A., Miura, K., Fay, M.P., Narum, D.L., Zhu, D., Mullen, G.E.D., Mahanty, S., Miller, L.H., Durbin, A.P., 2010. Phase 1 trial of Plasmodium falciparum blood stage vaccine MSP142-C1/Alhydrogel with and without CPG7909 in malaria naïve adults. PLoS ONE 5, 1–9, e8787.
Gesheva, V., Idakieva, K., Kerekov, N., Nikolova, K., Mihaylova, N., Doumanova, L., Tchorbanov, A., 2011. Marine gastropod hemocyanins as adjuvants of non-conjugated bacterial and viral proteins. Fish Shellfish Immunol. 30, 135–142.
Gherardi, R.K., Coquet, M., Cherin, P., Belec, L., Moretto, P., Dryfus, P.A., Pellissier, J.-F., Chariot, P., Authier, F.-J., 2001. Macrophage myofasiciitis lesions assess long-term persistence of vaccine-derived aluminium hydroxide in muscle. Brain 124, 1821–1831.
Glenny, A.T., Pope, C.G., Waddington, H., Wallace, U., 1926. The antigenic value of the toxoid precipitated by potassium alum. J. Pathol. Bacteriol. 29, 38–45.
Gravito, R.M., Rosenbusch, J.P., 1986. Isolation and crystallization of bacterial porin. Meth. Enzymol. 125, 309–328.
Guo, D., Wang, H., Zeng, D., Li, X., Fan, X., Yongdong, L., 2011. Vaccine potential of hemocyanin from *Oncomelania hupensis against Schistosoma japonium*. Parasitol. Int. 60, 242–246.
Harris, A.B., 1973. Ultrastructure and histochemistry of alumina in cortex. Exp. Neurol. 38, 33–63.
Harris, J.R., 1997. Negative Staining and Cryoelectron Microscopy: The Thin Film Techniques. RMS Microscopy Handbook No. 35. BIOS Scientific Publishers, Oxford.
Harris, J.R., Markl, J., 1999. Keyhole limpet hemocyanin (KLH): a biomedical review. Micron 30, 597–623.
Harris, J.R., Scheffler, D., 2002. Routine preparation of air-dried negatively stained and unstained specimens on holey carbon support films: a review of applications. Micron 33, 461–480.
Hem, S.L., HogenEsch, H., 2007. Relationship between physical and chemical properties of aluminium-containing adjuvants and immunopotentiation. Expert Rev. Vaccines 6, 685–698.
Hem, S.L., HogenEsch, H., Middaugh, C.R., Volkin, D.B., 2010. Preformulation studies—the next advance in aluminium adjuvant-containing vaccines. Vaccine 28, 4868–4870.
Hernández, I., Sanmartin, O., Cardá, C., Gómez, S., Alfaro, A., 2008. B-Cell pseudolymphoma caused by aluminium hydroxide following hyposensitization therapy. Actas Dermosifiliogr. 99, 213–216.
Hochepied, J.-F., Ilioukhina, O., Berger, M.-H., 2003. Effect of the mixing procedure on aluminium(oxide)-hydroxide obtained by precipitation of aluminium nitrate with soda. Mater. Lett. 57, 2817–2822.
Janney, D.E., Cowley, J.M., Buseck, P.R., 2000. Transmission electron microscopy of synthetic 2- and 6-line ferrihydrate. Clays Clay Miner. 48, 111–119.
Johnston, C.T., Wang, S.-L., Hem, S.L., 2002. Measuring the surface area of aluminium hydroxide adjuvant. J. Pharm. Sci. 91, 1702–1706.
Jones, L.S., Peek, L.J., Power, J., Markham, A., Yazzie, B., Middaugh, C.R., 2005. Effects of adsorption to aluminium salt adjuvants on the structure and stability of model protein antigens. J. Biol. Chem. 280, 13406–13414.
Lee, S.O., Jung, H.K., Oh, C.J., Lee, Y.H., Tran, T., Kim, M.J., 2009. Precipitation of fine aluminium hydroxide from Bayer liquors. Hydrometallurgy 98, 156–161.
Leonelli, C., Mason, T.J., 2010. Microwave and ultrasonic processing: now a realistic option for industry. Chem. Eng. Process. 49, 885–900.
Li, Z., Tao, X., Cheng, Y., Wu, Z., Zhang, Z., Dang, H., 2007. A facile way for preparing tin nanoparticles from bulk tin via ultrasound dispersion. Ultrason. Sonochem. 14, 89–92.
Li, Y., Zhang, Y., Yang, C., Zhang, Y., 2009. Precipitating sandy aluminium hydroxide from sodium aluminate solution by the neutralization of sodium bicarbonate. Hydrometallurgy 98, 52–57.
Li, Y., Zhang, Y., Yang, C., Chen, L., Zhang, Y., 2010. Crystallization of aluminium hydroxide from the reactive $NaAl(OH)_4$–$NaHCO_3$ solution: experiment and modeling. Chem. Eng. Sci. 65, 4906–4912.
Lindblad, E.B., 2004. Aluminium adjuvants—in retrospect and prospect. Vaccine 22, 3658–3668.
Lindblad, E.B., 2006. Mineral adjuvants. In: Immunomodulators in Modern Vaccines, pp. 217–233.
MacLellan, K., Loney, C., Yeo, R.P., Bhella, D., 2007. The 24-Angstrom structure of respiratory syncytial virus nucleocapsid protein-RNA decameric rings. J. Virol. 81, 9519–9524.
McLaughlin, W.J., White, J.L., Hem, S.L., 1993. Heterocoagulation in magnesium hydroxide and aluminium hydroxycarbonate suspensions. J. Colloid Interf. Sci. 157, 113–123.
Miller, J., Willamson, E.D., Lakey, J.H., Titball, R.W., 1998. Macromolecular organisation of recombinant *Yersinia pestis* F1 antigen and the effect of structure on immunogenicity. FEMS Immunol. Med. Microbiol. 212, 13–22.
Mortimer, R.J., Mayes, R.J., 2007. Characterisation and humidity-sensing properties of aluminium (oxy-hydroxide films prepared by cathodically induced precipitation. Sens. Actuators B 128, 124–132.
Mueller, C.A., Broz, P., Müller, S.A., Ringer, P., Erne-Brand, F., Sorg, I., Kuhn, M., Engel, A., Cornelis, G.R., 2005. The V-antigen of *Yersina* forma a distinct structure at the tip of injectisome needles. Science 310, 674–676.
Mullen, G.E.D., Giersing, B.K., Ajose-Popoola, O., Davis, H.L., Kothe, C., et al., 2006. Enhancement of functional antibody responses to AMA1-C1/Alhydrogel^c, a *Plasmodium falciparum* malaria vaccine, with CpG oligodeoxynucleotide. Vaccine 24, 2497–2505.
Nguyen, V.S., Rouxel, D., Hadji, R., Vincent, B., Fort, Y., 2011. Effect of ultrasonication and dispersion stability on the cluster size of alumina nanoscale particles in aqueous solutions. Ultrason. Sonochem. 18, 382–388.
Petosa, C., Collier, R.J., Klimpel, K.R., Leppla, S.H., Liddington, R.C., 1997. Crystal structure of the anthrax toxin protective antigen. Nature 385, 833–838.
Presicce, P., Taddeo, A., Conti, A., Villa, M.L., Bella, S.D., 2008. Keyhole limpet hemocyanin induces the activation and maturation of human dendritic cells through the involvement of mannose receptor. Mol. Immunol. 45, 1136–1145.
Rinella, J.V., White, J.L., Hem, S.L., 1996. Treatment of aluminium hydroxide adjuvant to optimise the adsorption of basic proteins. Vaccine 14, 298–300.
Rostenberg, M., Remarque, E., de Jong, E., Hermsen, R., Blythman, H., et al., 2008. Safety and Immumnogenicity of a recombinant Plasmodium falciparum AMA1 malaria vaccine adjuvinated with Alhydrogel^{TM}, montanide ISA 720 or AS02. PLoS ONE e3960, 1–12.
Sagara, I., Dicko, A., Ellis, R.D., Fay, M.P., Diawara, S.I., et al., 2009. A randomized controlled phase 2 trial of the blood stage AMA1-Ca/Alhydrogel malaria vaccine in children in Mali. Vaccine 27, 3090–3098.
Sato, T., 2007. Preparation and Characterization of Aluminium Hydroxides and Aluminas. Litarvan Literature, USA.
Shirodkar, S., Hutchinson, R.L., Perry, D.L., Whjite, J.L., Hem, S.L., 1990. Aluminium compounds used as adjuvants in vaccines. Pharm. Res. 7, 1282–1288.
Shurig, H., Rutkat, K., Rachel, R., Jaenicke, R., 1995. Octameric enolase from the hyperthermophilic bacterium *Thermotoga maritime*: purification, characterization, and image processing. Protein Sci. 4, 228–236.
Soliakov, A., Harris, J.R., Watkinson, A., Lakey, J., 2010. The structure of *Yersinia pestis* Caf1 polymer in free and adjuvant bound states. Vaccine 28, 5746–5754.
Solanki, V.A., Jain, N.K., Roy, I., 2011. Stabilization of tetanus toxoid formulation containing aluminium hydroxide adjuvant against freeze-thawing. Int. J. Pharm. 414, 140–147.
Tawar, R.G., Duquerroy, S., Vonrhein, C., Varela, P.F., Damier-Piolle, L., Castagné, N., CacLellan, K., Bedouelle, H., Bricogne, G., Bhella, D., Eléouët, J.-F., Rey, F.A., 2009. Crystal structure of a nucleocapsid-like nucleoprotein-RNA complex of respiratory syncytial virus. Science 326, 1279–1283.
Valtulini, S., Macchi, C., Ballanti, P., Cherel, Y., Laval, A., Theaker, J.M., Bak, M., Ferretti, E., Morvan, H., 2005. Aluminium hydroxide-induced granuloma in pigs. Vaccine 23, 3999–4004.
Wang, D.-G., Guo, F., Chen, J.-F., Zhao, R.-H., Zhang, Z.-T., 2008. Synthesis of nanoplatelets of modified aluminium hydroxide by high gravity reactive precipitation and hydrothermal method. Mater. Chem. Phys. 107, 426–430.
Wolff, L., Flemming, J., Schmitz, R., Gröger, Müller-Goymann, C., 2008. Protection of aluminium hydroxide during lyophilization as an adjuvant for freeze-dried vaccines. Coll. Surf. A: Physicochem. Eng. Aspects 330, 116–126.
Wu, Z., Wang, D., Liang, X., Sun, A., 2011. Ultrasonic-assisted preparation of metastable hexagonal MoO3 nanorods and their transformation to microbelts. Ultrason. Sonochem. 18, 288–292.
Yamashita, E., Zhalnia, M.V., Zakharov, S.D., Sharma, O., Cramer, W.A., 2008. Crystal structures of the OmpF porin: function in a colicin translocon. EMBO J. 27, 2171–2180.
Zavialov, A.V., Berglund, J., Pudney, A.F., Fooks, L.J., Ibrahim, T.M., Macintyre, S., Knight, S.D., 2003. Structure and biogenesis of the capsular F1 antigen from *Yersina pestis*: preserved folding energy drives fiber formation. Cell 113, 587–596.
Zhang, C., Wei, D., Liu, Z., Liao, T., Zhang, C., 2010. Synthetic peptide coupled to KLH elicits antibodies against beta8 integrin. Hybridoma 4, 361–366.
Zhu, D., Huang, S., Gebregeorgis, E., McClellan, H., Dai, W., Miller, L., Saul, A., 2009a. Development of a direct alhydrogel formulation immunoassay (DAFIA). J. Immunol. Methods 344, 73–78.
Zhu, D., Saul, A., Huang, S., Martin, L.B., Miller, L.H., Rausch, K.M., 2009b. Use of *o*-phthalaldehyde assay to determine protein contents of Alhydrogel-based vaccines. Vaccine 27, 6054–6059.